



Alfvénic plasma velocity variations observed at the inner edge of the low-latitude boundary layer induced by the magnetosheath mirror mode waves: A THEMIS observation

M. Nowada,¹ J.-H. Shue,¹ C.-H. Lin,² T. Sakurai,³ D. G. Sibeck,⁴ V. Angelopoulos,⁵ C. W. Carlson,⁶ and H.-U. Auster⁷

Received 31 December 2008; revised 12 April 2009; accepted 4 May 2009; published 9 July 2009.

[1] With unique simultaneous observations both in the magnetosheath and magnetosphere by the THEMIS probes, Alfvénic variations in the plasma velocity are observed at the inner edge of low-latitude boundary layer (LLBL) and are induced by the mirror mode waves in the magnetosheath near the subsolar magnetopause on 31 July 2007. These Alfvénic variations appeared as the wavy perturbations in the V_x and V_y components observed by THEMIS C, D, and E, which had the same periodicity as associated magnetic field variations. Simultaneously, THEMIS B observed the mirror mode waves in the magnetosheath. The periodicities of the magnetic and plasma pressure variations of mirror modes in the magnetosheath were consistent with those of the Alfvénic wavy variations in the LLBL. Therefore, the mirror mode waves can induce the magnetopause undulations, launching Alfvén waves, and resultant Alfvénic variations are observed in the LLBL. Also, in the succeeding magnetosheath interval by THEMIS B, we examined whether the mirror mode waves occurred and associated Alfvénic variations were observed in the LLBL. However, no clear evidence for an existence of the mirror mode waves was obtained, and THEMIS C, D, and E do not also observe associated magnetic field and plasma Alfvénic responses in the LLBL. These results suggest that the Alfvénic variations in the LLBL are strongly related to the mirror mode waves in the magnetosheath. On the basis of these results, we emphasize that the magnetosheath energy is transmitted and transported into the magnetosphere via magnetopause surface waves.

Citation: Nowada, M., J.-H. Shue, C.-H. Lin, T. Sakurai, D. G. Sibeck, V. Angelopoulos, C. W. Carlson, and H.-U. Auster (2009), Alfvénic plasma velocity variations observed at the inner edge of the low-latitude boundary layer induced by the magnetosheath mirror mode waves: A THEMIS observation, *J. Geophys. Res.*, 114, A07208, doi:10.1029/2008JA014033.

1. Introduction

[2] Many magnetic field and plasma variations observed in the magnetosphere and the magnetospheric boundary layers are caused by the variations of solar wind conditions [e.g., Sibeck *et al.*, 1989a, 1989b; Kivelson and Southwood, 1991]. In particular, these magnetospheric variations appear as “waves,” and there is a good correlation between the periodicity of the waves and that of the solar wind pressure

variations [e.g., Kim *et al.*, 2002]. When the solar wind dynamic pressure suddenly changes, the magnetopause starts to move, and associated waves are launched on its surface. The induced surface waves, in turn, launch fast, slow, and Alfvén mode waves, propagating upon the magnetopause and the magnetospheric boundary layers. Resultant signatures are detected as magnetic field and plasma perturbations [e.g., Glassmeier *et al.*, 2008].

[3] Matsuoka *et al.* [1995], Kim *et al.* [2002], and Kessel [2008] demonstrated the magnetospheric response to periodic solar wind dynamic pressure variations. From their results, ultralow frequency (ULF) waves with Pc 5 range or Pi 3 irregular pulsations with irregular waveform and periods were observed as the responses in the magnetosphere and on the ground to periodic variations of the solar wind dynamic pressure. Long-period magnetic irregular pulsations (i.e., Pi 3) driven by the solar wind pressure variations can propagate into the dayside and nightside magnetosphere, although the detailed propagation mechanism remains an open question [Matsuoka *et al.*, 1995]. Kessel [2008] examined the direction of the Poynting flux along the magnetopause surface, and showed that almost all of the Poynting flux (about 70%) was directed inward. From

¹Institute of Space Science, National Central University, Zhongli, Taiwan.

²Department of Electrical Engineering, Ching Yun University, Zhongli, Taiwan.

³Department of Aeronautics and Astronautics, Tokai University, Hiratsuka, Japan.

⁴NASA Goddard Space Flight Center, Greenbelt, Maryland, USA.

⁵Institute of Geophysics and Planetary Physics, University of California, Los Angeles, California, USA.

⁶Space Sciences Laboratory, University of California, Berkeley, California, USA.

⁷Institut für Geophysik und Extraterrestrische Physik, Technische Universität, Braunschweig, Germany.

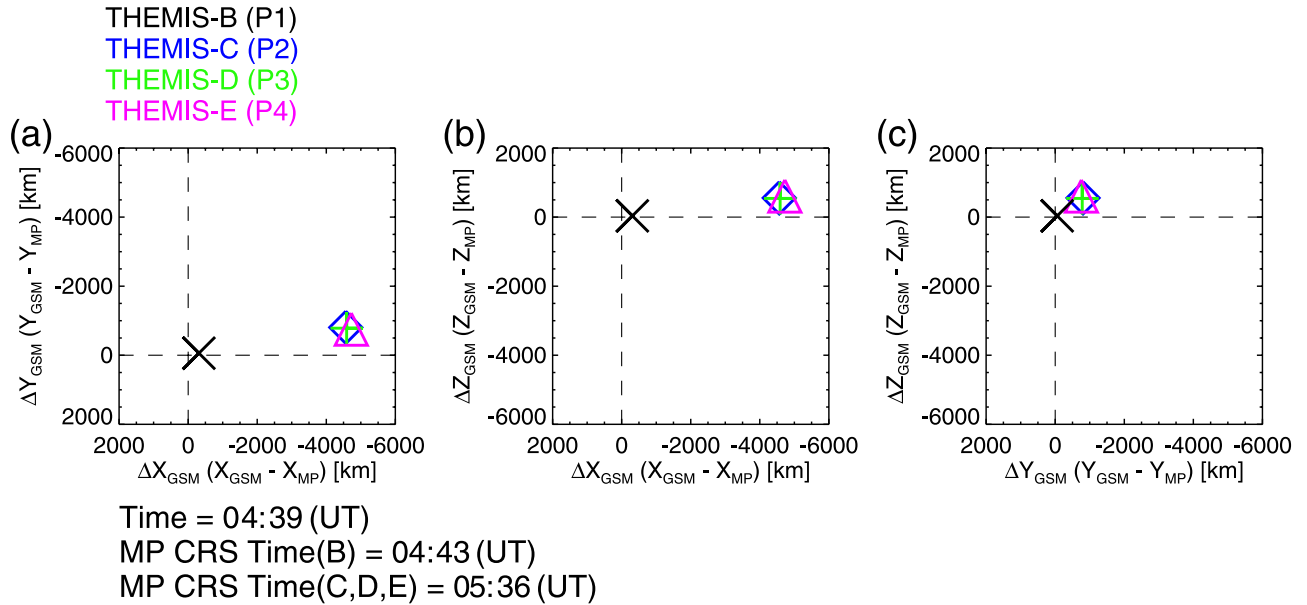


Figure 1. The relative positions of four THEMIS probes (THEMIS B (P1), C (P2), D (P3), and E (P4)) from the dayside magnetopause at 0439 UT on 31 July 2007 are plotted. The relative positions of THEMIS B, C, D, and E from the dayside magnetopause (the probe position minus the location of the dayside magnetopause) projected onto (a) GSM XY, (b) GSM XZ, and (c) GSM YZ are shown. The positions of THEMIS B, C, D, and E are shown with black cross, blue diamond, green plus, and magenta triangle, respectively.

this result, the solar wind energy is also transmitted into the magnetosphere through the magnetopause surface waves.

[4] There are also waves in the magnetosheath adjacent to the magnetopause. When β (the ratio between the plasma and the magnetic pressures) > 1 and $\frac{T_{\perp}}{T_{\parallel}} > 1$, mirror mode waves frequently occur [Tsurutani *et al.*, 1982; Lucek *et al.*, 1999a, 1999b, 2001]. Cattaneo *et al.* [1998], Joy *et al.* [2006] and Violante *et al.* [1995] reported that enhanced mirror mode wave amplitudes approaching the magnetopause. Song *et al.* [1992a, 1992b] pointed out that the dynamic energy of the mirror mode waves in the magnetosheath could contribute to the power in the other wave modes both in the magnetosheath and the magnetosphere.

[5] The present study uses both the magnetic field and plasma data obtained by the THEMIS spacecraft with a unique “string-of-pearls” configuration, to examine how the magnetic field and plasma on the magnetospheric side respond to waves observed in the magnetosheath near the magnetopause. This study is very important to understand how the solar wind energy is transmitted via waves. This study describes waves which were observed under the northward IMF and quiet solar wind conditions. THEMIS C, D and E were located at the inner edge of the dawnside LLBL near the subsolar region. They observed wavy variations with a period from 0.5 minute to 1 minute in the X and Y components of the plasma velocity. Interestingly, associated fluctuations did not appear in the plasma density and the temperature. The simultaneously observed magnetic field exhibited similar periodic variations. Furthermore, the magnetic field and plasma wavy variations were in phase. Meanwhile, THEMIS B observed mirror mode waves which can induce the magnetopause undulations, launching the compressive and Alfvén mode waves.

[6] We examined the relationships between the wavy velocity variations observed at the inner edge of LLBL and the mirror mode waves observed in the magnetosheath. As a result, we can provide a detailed picture of the magnetic field and plasma responses from the magnetosheath to the magnetosphere.

2. Instrumentation

[7] The THEMIS mission consists of five satellites which were launched on 17 February 2007, to reveal the spatial-temporal structures of magnetospheric processes (see details in the work by Angelopoulos [2008]). In the present study, we used the magnetic field data obtained from the fluxgate magnetometers (FGM) that is capable of measuring the low-frequency fluctuations up to 64 Hz, and detecting the magnetic field variations within an accuracy of ± 0.01 nT [Auster *et al.*, 2008]. Also, we utilized the plasma moment data from electrostatic analyzer (ESA) with the observable range for ions between 0.006 keV/q and 20 keV/q [McFadden *et al.*, 2008] onboard all five probes of THEMIS spacecraft. The time resolutions of both the magnetic field and plasma moment data are 3 s. On 31 July 2007, the THEMIS fleet was in the Injection and Coast phase with a string-of-pearls configuration, in which all of five probes were on the same orbit with an apogee of 14.7 Re and a perigee of 1.16 Re.

3. Locations of THEMIS’s Four Probes

[8] Figure 1 shows the relative positions of THEMIS B (P1), C (P2), D (P3) and E (P4) from the dayside magnetopause (the probe position minus the location of the

dayside magnetopause) at 0439 UT on 31 July 2007, projected onto XY (Figure 1a), XZ (Figure 1b) and YZ (Figure 1c) planes in the geocentric solar magnetospheric (GSM) coordinate system. The positions of THEMIS B, C, D and E are marked with black cross, blue diamond, green plus and magenta triangle, respectively. The magnetopause location was determined by the magnetopause crossing from the magnetosheath to the magnetosphere, which THEMIS B experienced at 0443 UT. This magnetopause crossing occurred just after THEMIS C, D, and E observed the wavy plasma velocity variations at the inner edge of LLBL at 0439 UT. THEMIS C, D, and E also observed the magnetopause in almost the same location at 0536 UT. A clear jump of the north–south magnetic field component (GSM B_z component) was used to identify the magnetopause crossing. The positions of THEMIS C, D and E were very close each other, and located the distance of 4000 km from the magnetopause on GSM X. The distance between THEMIS C and D was 200 km \sim 250 km, and that between THEMIS C, D and E was 600 km \sim 1000 km on GSM all planes. THEMIS B was very close to the magnetopause, and the distance between THEMIS B and THEMIS C, D, E was also about 4000 km. However, there were no latitudinal and longitudinal differences between THEMIS B and C, D, and E.

4. Solar Wind Condition

[9] We begin by examining how simultaneous solar wind conditions varied. The wavy plasma velocity variations in LLBL, focused in this study occurred during the midterm of a long-lasting high-speed stream (29 July to 5 August 2009). During the interval of high-speed stream, the average solar wind speed was about 540 km/s, and the dynamic pressure was highly variable from 0.6 nPa and 1.0 nPa (the long-term plots for the solar wind parameters are not shown here.) We zoomed in and examined the corresponding solar wind conditions to the wavy velocity variations in LLBL.

[10] Figure 2 shows a 3-h summary plot of the solar wind parameters that were obtained from the ACE spacecraft. From top to bottom, three components of IMF (B_x , B_y and B_z) in GSM coordinates, the magnetic field intensity (B_t), and the solar wind dynamic pressure (P_d) are plotted versus universal time. The time resolutions of the magnetic field and plasma moment data are 16 s and 64 s, respectively. These time resolutions are the most accurate in the distributed data. The convection time of the solar wind (i.e., time lag between THEMIS and ACE) was 48 min, estimated by the formula proposed by *Hsu and McPherron* [2003]. The intervals during which THEMIS observed the waves in the magnetosheath and did not observe them were bracketed by two vertical black lines and two gray solid lines, respectively. During the whole interval, all components of the magnetic field were fluctuating. In particular, the small frequent fluctuations whose frequency was between 3.2 mHz and 6.4 mHz were observed on the B_t during the 1.5-h interval between 0200 and 0330 UT. However, the frequent variations of the magnetic field intensity corresponding to the magnetosheath wave structures were not observed in the B_t . Simultaneous IMF directions were sunward ($+B_x$), dawnward ($-B_y$) and northward ($+B_z$) directions. The small fluctuations with the frequency between 6.4 mHz and 8.5 mHz were also found on the B_t

during which the wavy plasma variations were absent. Simultaneous directions of the IMF were sunward ($+B_x$), dawnward ($-B_y$) and almost southward ($-B_z$). The dynamic pressure also did not show the drastic variations, and has been almost stable during whole interval. Furthermore, there was no clear difference between the average values of the dynamic pressure during the magnetosheath wave structures were observed and not observed (about 0.45 nPa).

5. Event on 31 July 2007

5.1. An Overview

[11] Figure 3 shows a summary plot of the magnetic field and the plasma moment data obtained from THEMIS C (blue), D (green), E (magenta), and B (black) during the interval of 52 min from 0421 to 0513 UT on 31 July 2007. THEMIS C, D and E observed the wavy plasma velocity variations at the inner edge of LLBL near the subsolar region during the interval of 5 min between 0435:30 and 0440:30 UT as bracketed by two cyan vertical solid lines. From top to bottom, three components of the magnetic field (B_x , B_y and B_z), the magnetic field strength (B_t), those of the plasma velocity (V_x , V_y and V_z) in GSM coordinates, the plasma number density (N_p) and the temperature (T) are shown. After 0506:30 UT, THEMIS D and E were lacking in the plasma data, and there was also a lack of plasma velocity data from THEMIS B. The interesting point on this phenomenon is that the wavy variations were particularly observed in the plasma velocity, but not in the plasma number density and the temperature. In the magnetic field component, the small amplitude variations were observed in association with these wavy plasma velocity variations (details are shown in Figure 4). The wavy variations were mainly found in both the V_x and V_y components, and were not observed in the V_z component. This indicates that the wavy velocity variations were the azimuthal and transverse waves, which were independent on the variations of both the plasma density and the temperature. The waves, detected by THEMIS C and D, had almost the same periods (\sim 1 minute) and amplitudes (70 km/s \sim 100 km/s). There was also nearly 90° phase difference between the V_x and V_y components. This indicates that hodograms are circular with a clockwise rotation of the V_x and V_y components. Although THEMIS E also observed the wavy variations, their amplitude was smaller than that observed by THEMIS C and D (20 km/s \sim 50 km/s). After 0440:30 UT, THEMIS C, D, and E did not observe both the wavy plasma or magnetic field variations.

[12] While THEMIS C, D and E observed the wavy variations in the plasma velocity at the inner edge of LLBL, THEMIS B was located in the magnetosheath just near the magnetopause as bracketed with navy vertical dashed lines in Figure 3. THEMIS B entered the magnetosheath from the magnetospheric side at 0430:00 UT, and has stayed there until 0443:14 UT. In the magnetosheath, THEMIS B observed the periodic magnetic field oscillations in both the B_z component and the magnetic field intensity with a period from 0.5 minute to 1 minute. Furthermore, these oscillations biased to positive values, and the intensity of the background magnetic field seemed to be similar to the magnetic field intensity in the magnetosphere. The variations of the magnetic field B_z component and the magnetic

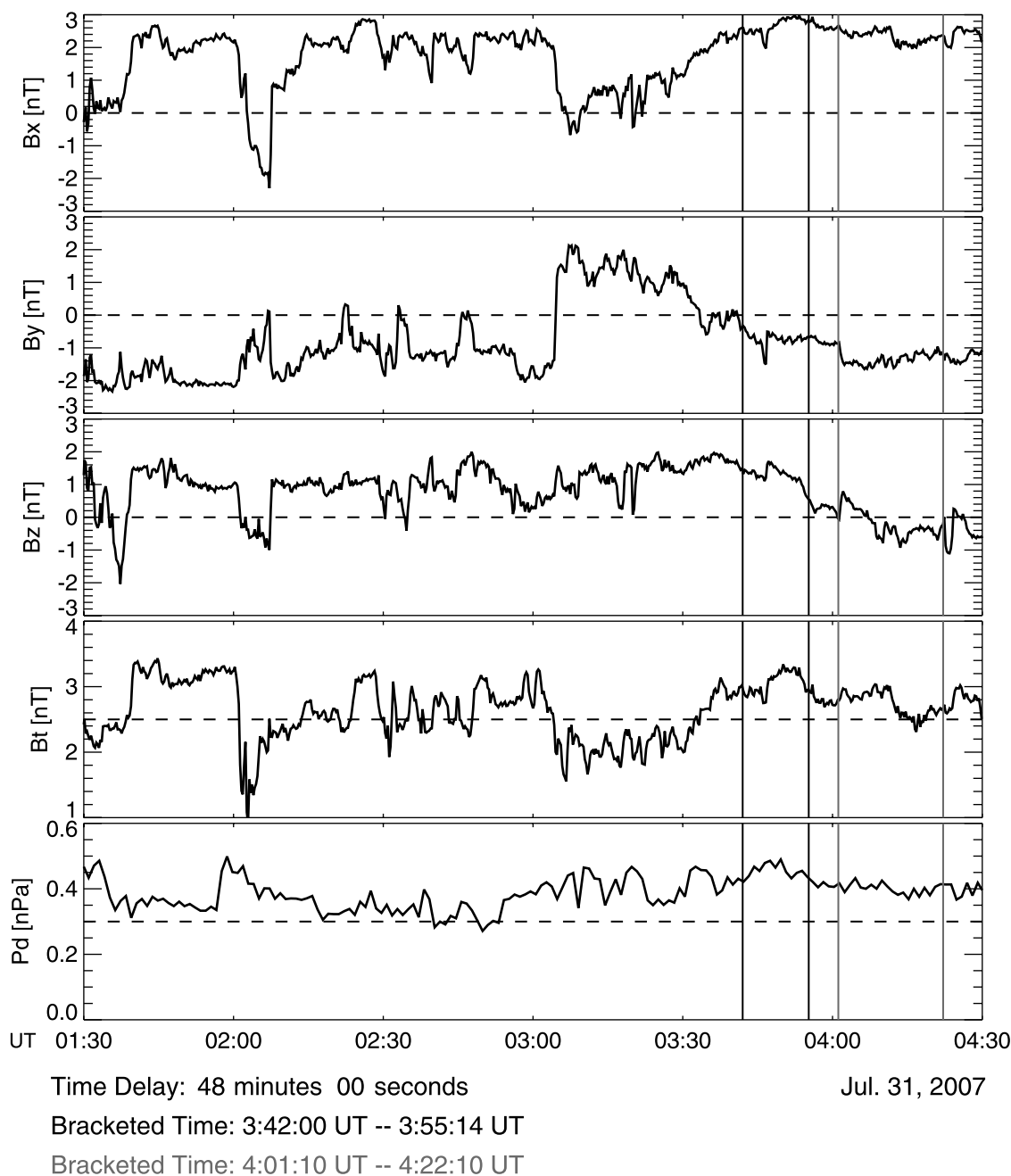


Figure 2. Plots of the solar wind conditions observed by the ACE spacecraft during the interval of the 3 h between 0130 and 0430 UT are shown. From top to bottom, three components of the IMF (B_x , B_y , and B_z) in GSM coordinates; the magnetic field intensity (B_t); and the solar wind dynamic pressure (P_d) are plotted versus universal time. The intervals during which THEMIS observed and did not observe the wave structures in the magnetosheath are bracketed by two black and two gray vertical solid lines, respectively. The time delay between ACE and THEMIS was about 48 min.

field intensity varied just out of phase to those for the plasma density and the temperature. The plasma density and temperature variations were in phase. The lower limit of the temperature was also the same as the temperature in the inner magnetosheath. The clear antiphase relation between the magnetic field and the plasma density provides evidence for waves in the magnetosheath just outside of the magnetopause. The characteristics of these observed waves resembled the slow mode (diamagnetic) or drift mirror waves.

THEMIS B reentered the magnetosphere at 0443:14 UT. All components of the plasma velocity fluctuate in both the magnetosphere and the magnetosheath. This would be the magnetospheric response to the waves observed in the magnetosheath. After 0443:14 UT, THEMIS B experienced two more magnetopause crossings. During the 21 min interval between 0449:10 and 0510:10 UT, THEMIS B observed the magnetosheath. However, the whole magnetic field and plasma variations were different from those in the

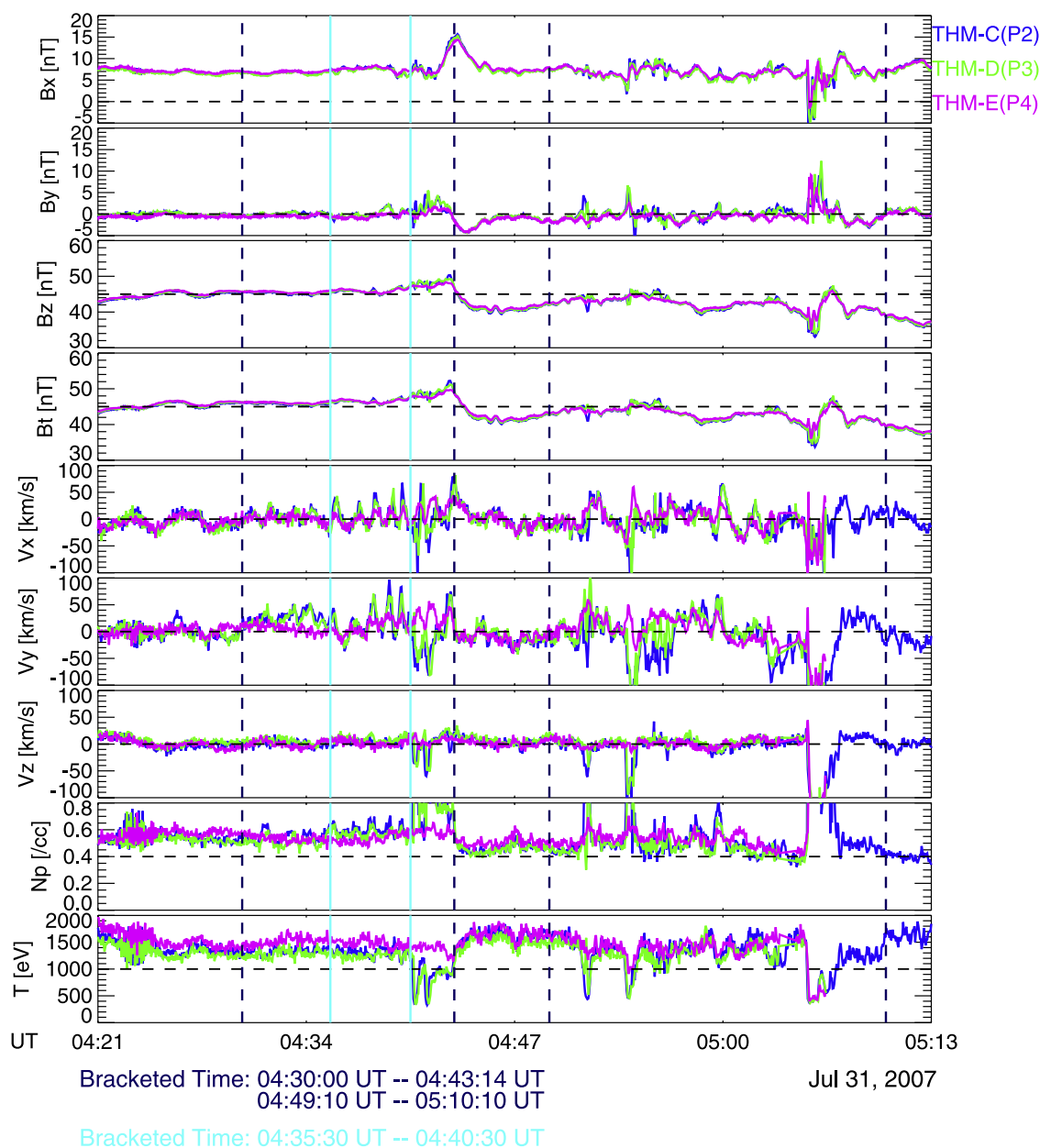


Figure 3. A summary plot of the observations by THEMIS C (blue), D (green), E (magenta), and B (black) during the interval of 52 min between 0421 and 0513 UT on 31 July 2007. From top to bottom, three components of the magnetic field (B_x , B_y , and B_z), the magnetic field strength (B_t), three plasma velocity components (V_x , V_y , and V_z) in GSM coordinates, the plasma number density (N_p), and the temperature (T) are shown. These parameters are plotted with universal time. After 0506:30 UT, THEMIS D and E were lacking in plasma data, and there was also a lack of plasma velocity data from THEMIS B. The interval during which the wavy velocity variations were observed is bracketed by two cyan vertical solid lines. The intervals that THEMIS B observed the magnetosheath twice are also bracketed by four navy vertical dashed lines.

previous magnetosheath interval, and the clear wave structures were not also observed in the magnetic field, the plasma density and the temperature. In particular, the fluctuations of the B_z component were much smaller, and ranged near 0 nT and in negative values. The corresponding THEMIS C, D, and E plasma velocity observations in the magnetospheric side did not show wavy variations. After 0510:10 UT, THEMIS B reentered the magnetosphere,

where the temperature was fluctuating as well as the previous entry of the magnetosphere at 0443:14 UT.

5.2. Magnetic Field Perturbations Associated With the Wavy Velocity Variations

[13] We removed the background values for the magnetic field, the plasma velocity and density to examine the small amplitude perturbations in greater detail. In order to subtract the background values from the observed those, we

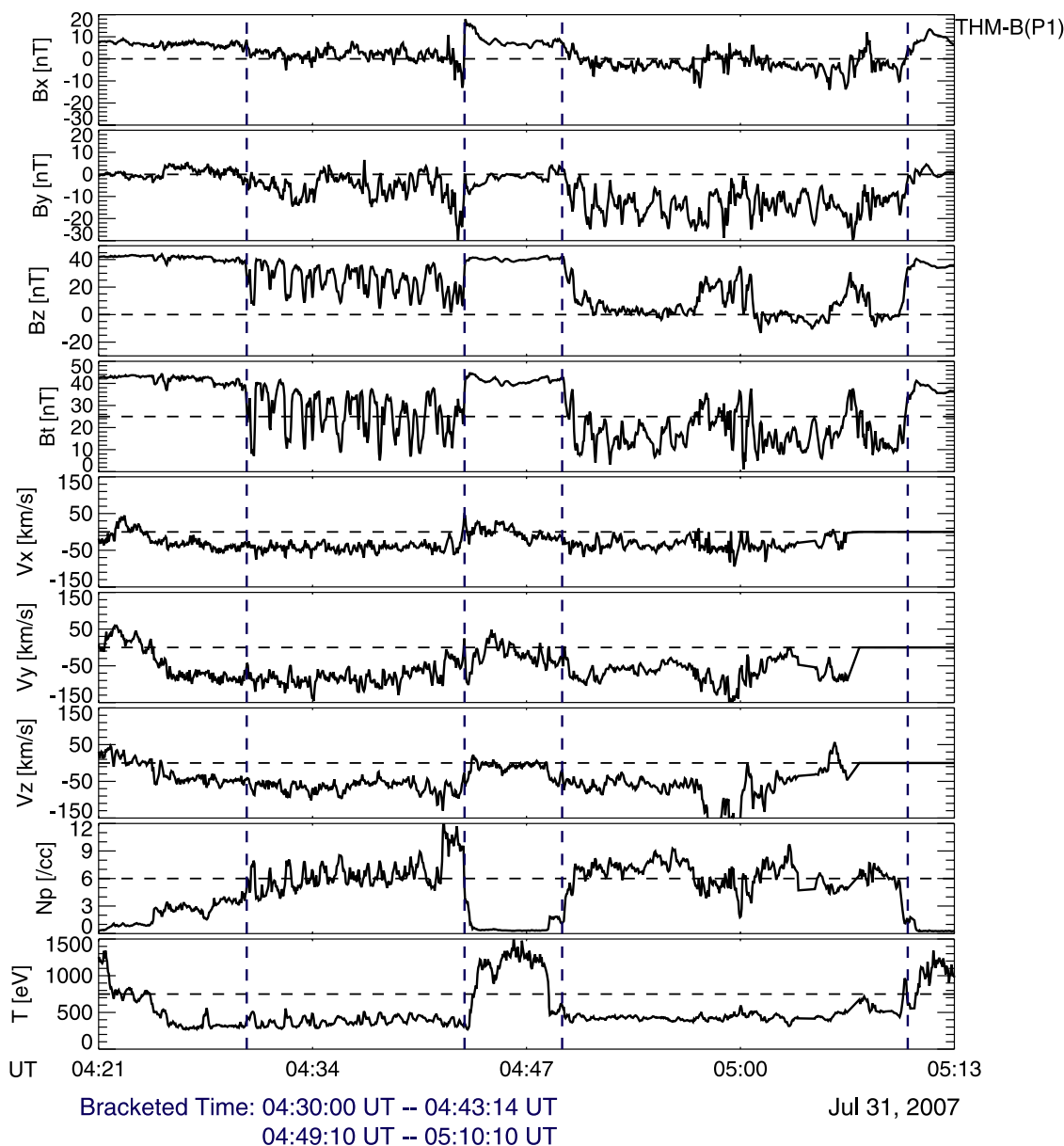


Figure 3. (continued)

introduced an equation of $\delta\mathbf{A} = \mathbf{A} - \langle\mathbf{A}\rangle$, where \mathbf{A} are observed values and $\langle\mathbf{A}\rangle$ are the averages over the 6 min interval between 0435 and 0441 UT. From top to bottom, the plots in Figure 4 show the fluctuations of three magnetic field components (δB_x , δB_y and δB_z), the magnetic field strength (δB_t), the plasma density (δN_p) and three plasma velocity components (δV_x , δV_y and δV_z). The magnetic field fluctuated within the range of ± 2.0 nT, and simultaneous velocity amplitudes ranged between -45 km/s and $+90$ km/s. Both the B_x and B_y components observed by THEMIS C and D exhibited greater variations than the B_z variation. Since the magnetic field orientation was almost the GSM Z direction, the wavy variations occur in the component transverse to the local magnetic field line. The variations of the plasma density were fluctuating with higher frequency than the magnetic field and plasma veloc-

ity, but not vary periodically. Also, these are independent on those of both the magnetic field and the plasma velocity. Meanwhile, simultaneous THEMIS E did not observe the small fluctuations of the magnetic field in association with the wavy velocity variations. The plasma density had little fluctuations during this interval.

6. Properties as Waves of the Plasma Velocity Variations

6.1. Relationship Between the Magnetic Field and Plasma Velocity

[14] In this section, we examine the properties as waves of the frequent velocity variations. In Figure 4, it seemed that the magnetic field did not vary in association with the wavy velocity variations. To investigate detailed relation-

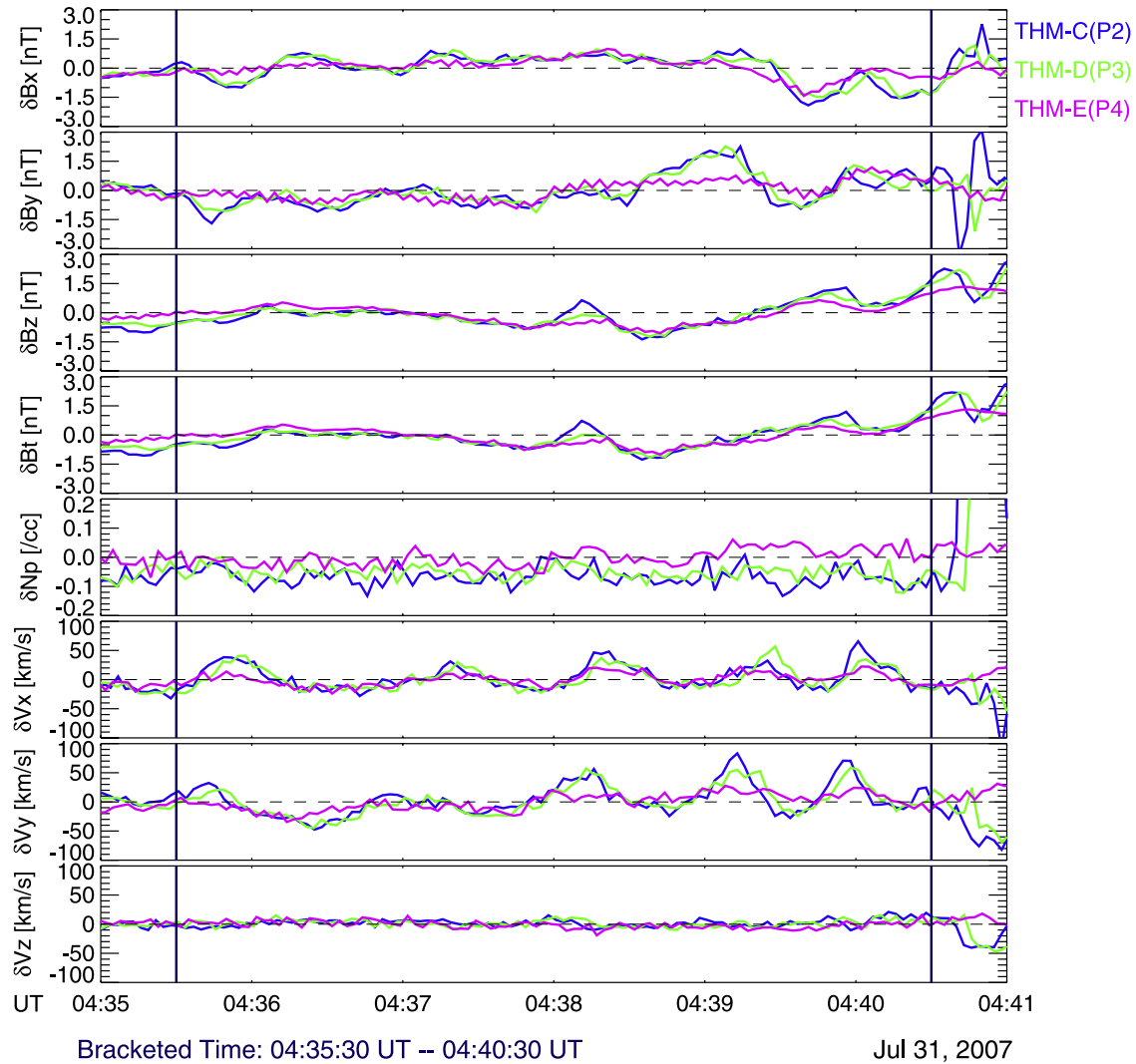


Figure 4. The fluctuations of the magnetic field, the plasma velocity, and the plasma density during the 6 min interval between 0435 and 0441 UT are shown. From top to bottom, the fluctuating of three magnetic field components (δB_x , δB_y , and δB_z), the magnetic field strength (δB_t), the plasma density (δN_p), and three plasma velocity components (δV_x , δV_y , and δV_z) are plotted. The fluctuations for each parameter were calculated by $A - \langle A \rangle$, where A are observed values, and $\langle A \rangle$ are the averages over this interval.

ship between these variations, the power spectra and the ellipticity were calculated on the basis of the magnetic field and the plasma velocity during the wavy velocity variations observed by THEMIS C and D, and the results are summarized in Table 1. The power spectra and ellipticity versus the wave frequency were calculated by using an autoregressive (AR) method which calculates the spectral parameters by fitting an autoregressive model to a time series. The detailed information on the AR method, including more excellent points than the classical spectral method, such as fast Fourier transform (FFT) is described by *Sakurai et al.* [1999]. The value of ellipticity was introduced to evaluate the shape of hodogram quantitatively. The shape of hodogram becomes liner if the ellipticity value is closer to 0. On the other hand, if the ellipticity is closer to 1, the hodogram

shape becomes circular. The sign of the ellipticity means the polarization of the hodogram, namely positivity and negativity denote the left- and right-handed polarizations, respectively.

[15] The values of common dominant frequency, which is the wave frequency corresponding to the peak of the power spectrum, between B_x and B_y observed by THEMIS C and D were almost the same (16.0 mHz \sim 17.0 mHz). The direction of the hodogram was also left handed because the values of ellipticity at the common dominant frequency were positive. The value of ellipticity in the magnetic field observed by THEMIS D is a little smaller than that by THEMIS C, but the shapes of the magnetic field hodograms were either almost circular because the ellipticity values were closer to 1 in both cases. Furthermore, the values of the common dominant frequency and

Table 1. Common Dominant Frequency and Corresponding Ellipticity Values of the Magnetic Field and Plasma Velocity During the Wavy Velocity Variations^a

Probes and Parameters	Dominant Frequency (mHz)	Ellipticity
THEMIS C ($B_x - B_y$)	17.0	+0.95
THEMIS C ($V_x - V_y$)	13.0	+0.95
THEMIS D ($B_x - B_y$)	16.0	+0.88
THEMIS D ($V_x - V_y$)	14.0	+0.91

^aEllipticity, the value closer to 0 means the liner hodogram and that closer to 1 shows the circular hodogram. Positive and negative signs denote the left- and right-handed polarizations, respectively.

those of ellipticity between V_x and V_y observed by THEMIS C and D were also almost the same (13.0 mHz \sim 14.0 mHz). These values were similar to those in the case of the magnetic field. The polarization and shape of the hodogram were also left handed and circular just as in the case of the magnetic field.

[16] From the values of the common dominant frequency and ellipticity, the magnetic field and plasma velocity were varying with the almost same frequency, and there were no phase differences between V_x and V_y , and between B_x and B_y during the wavy velocity variations.

[17] Next, we investigated the correlation between the magnetic field and the plasma velocity by calculating the cross power spectrum between these parameters. Simultaneously, we also calculated the phase angle and corresponding time delay between the magnetic field and plasma velocity with AR methods shown in Table 2. The values of common dominant frequency between the magnetic field and plasma velocity observed by THEMIS C and D were almost the same. Except for the relationship between B_x and V_x observed by THEMIS D, the phase differences were not observed because the time delays corresponding to the phase differences were within the time resolutions of the magnetic field and plasma velocity. However, the corresponding time delay between the B_x and V_x observed by THEMIS D was only 13 s (about 4 data points) even though the phase angle was much larger than the others. Therefore, the magnetic field and plasma velocity varied with not only the same frequency but also having in-phase relation.

6.2. An Estimation of Wave Mode of the Wavy Velocity Variations

[18] As seen in Figures 3 and 4, the variations of the magnetic field were independent on those of the plasma number density. To examine this independence quantitatively, we investigated the coherence and phase angle between the magnetic field strength and the plasma number density during the wavy velocity variations between 0435:30 and 0440:30 UT. We investigated in the case of THEMIS C. Figure 5 shows the plots of the coherence (Figure 5a) and the phase angle (Figure 5b) against the frequency. During this interval, the coherence was almost below 0.5, which is a threshold for good coherence between two parameters as shown with horizontal dashed line. At corresponding common dominant frequency between the magnetic field and plasma density variations (about 13.0 mHz) as shown with

vertical solid line, the coherence value was about 0.25. The simultaneous phase angle was very variable. If the wavy velocity variations have the characteristics of slow or fast mode wave, the phase angle between the magnetic field strength and the plasma density can be 180° (shown with horizontal dashed line) or 0° (shown with horizontal dotted line), respectively. Furthermore, the phase difference was about 70° at corresponding common dominant frequency.

[19] The wavy variations observed in the plasma velocity are traveling along the magnetic field line because the wavy variations appeared only in the V_x and V_y components. However, these wavy velocity variations are not “pure” fast or slow mode waves because there was no clear correlation between the magnetic field and the plasma density variations, and the plasma velocity and magnetic field were also varying with the same frequency. Furthermore, the wavy plasma variations are not pure Alfvén waves because no phase differences between the V_x and V_y components were observed. Therefore, the observed plasma velocity variations may be “mixed” mode wave structures, which the fast, slow and Alfvén mode waves intermingled complicately. We also examined which wave mode was the most dominant in this mixed mode structure.

[20] Figure 6 shows hodograms projected onto the plane of the velocities perpendicular to the local magnetic field line ($V_{\text{perp1}} - V_{\text{perp2}}$ plane) during the interval of 2.5 min between 0437:30 and 0440:30 UT. During this interval, the clearest wavy variations were observed in the plasma velocity. The direction of the magnetic field line is dominantly northward. From left to right, the hodograms for the plasma velocities observed by THEMIS C, D and E are plotted. The velocity hodograms from THEMIS C and D presented the clear vortex-like structures and left-handed (LH) polarizations. These results are consistent with the positive values of ellipticity of the plasma velocities near 1 observed by THEMIS C and D. Furthermore, these suggest that THEMIS C and D observed similar waves in the plasma velocity with a common source. These vortex-like structures observed by THEMIS C and D are evidence that these waves are traveling in the field-aligned direction, such as Alfvén waves. Accordingly, Alfvénic characteristics are the most dominant in observed mixed mode waves.

[21] In the velocity hodogram of THEMIS E, the scale range of the velocity hodogram was much smaller than those of both THEMIS C and D. Furthermore, no clear vortex-like hodogram with a LH polarization was found. This indicates that the waves observed by THEMIS E can be different from those observed by THEMIS C and D, and do not have Alfvénic characteristics. If one considers that the distance between THEMIS C, D and E was within

Table 2. Common Dominant Frequency, Phase Angle, and Corresponding Time Delay Between the Magnetic Field and Plasma Velocity During the Wavy Velocity Variations

Probes and Parameters	Dominant Frequency (mHz)	Phase Angle (deg)	Time Delay (s)
THEMIS C ($B_x - V_x$)	19.0	25.0	3.6
THEMIS C ($B_y - V_y$)	19.0	17.0	2.5
THEMIS D ($B_x - V_x$)	16.0	74.0	13.0
THEMIS D ($B_y - V_y$)	18.0	17.0	2.5

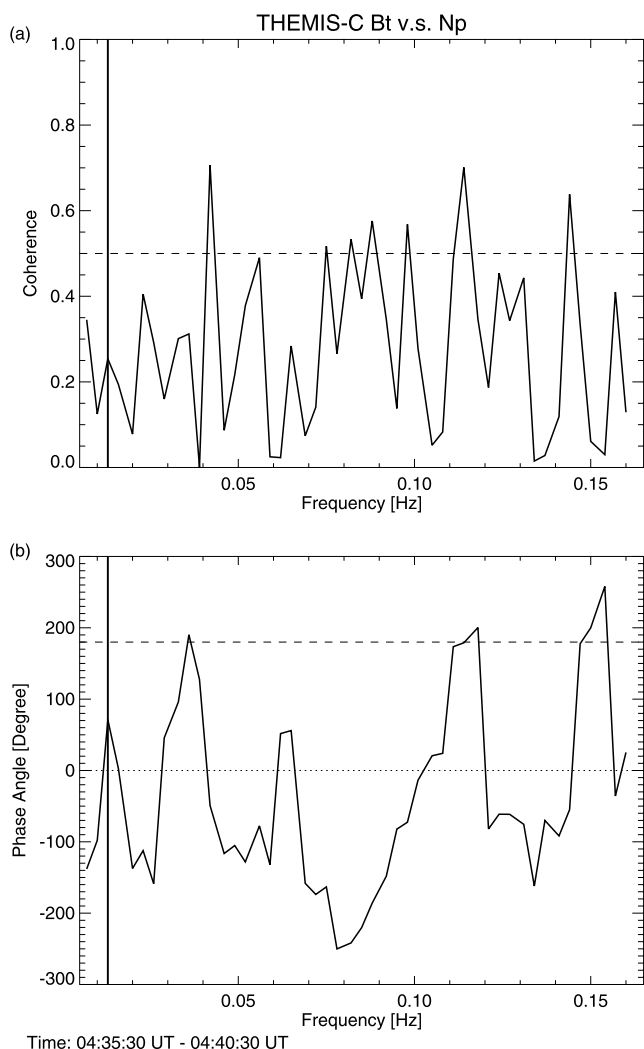


Figure 5. (a) The coherence and (b) the phase angle between the magnetic field strength and the plasma density obtained from THEMIS C during the wavy velocity variations from 0435:30 to 0440:30 UT was plotted against the wave frequency. The coherence value of 0.5 for a threshold of good coherence is shown with the horizontal dashed line in Figure 5a. The dashed and dotted lines in Figure 5b show the thresholds of the slow (180°) and fast (0°) mode waves.

1000 km, the wavy variations might occur in a narrow region.

7. Discussion

7.1. An Interpretation of and Possible Source for the Wavy Plasma Velocity Variations

[22] At the inner edge of the LLBL near the subsolar region, the wavy variations were observed in the plasma velocity. There were only small amplitude magnetic field variations, but the dominant frequency range was almost the same as that for the wavy velocity variations, and the phase difference between the magnetic field and plasma velocity was little. Therefore, the magnetic field varied in association with the wavy variations in the plasma velocity. On the

other hand, the plasma density and temperature did not show any associated periodic variations, and there was no clear correlation between the magnetic field and plasma number density variations. The hodograms on the plane of the velocities perpendicular to the magnetic field line had clear vortex-like structures, indicating that the waves are traveling in the field-aligned direction. Theoretically, the fast, slow and Alfvén mode waves are excited in the magnetosphere where the Alfvén velocity is the fastest wave speed, and traveling in the field-aligned direction (see Friedrichs diagram shown by *Kivelson and Russell* [1995, Figure 11.3]).

[23] However, the traveling direction of the wave energy, evaluated as the Poynting vector was almost field aligned. The magnetic field strength in the B_z component was the largest during the wavy variations, and the Z direction is approximately the field-aligned direction. The wavy plasma variations appeared in the V_x and V_y components, which are the perpendicular to the magnetic field. The V_x and V_y are also corresponding to E_y and E_x from the equation of frozen-in condition ($E = -V \times B$). Therefore, in the Z (field-aligned) direction, the wave energy are dominantly flowing on the basis of the equation of Poynting vector ($S = \frac{E \times B}{\mu_0}$). We conclude that the wavy plasma variations are almost “Alfvénic” from these results

[24] Next, we consider a possible source to cause these wavy variations. Simultaneous IMF direction and solar wind conditions provided no evidence for any drastic changes. Accordingly, variations of the solar wind conditions should be excluded as a possible cause. However, during the interval of the wavy velocity variations, THEMIS B simultaneously observed some periodic magnetic field fluctuations in the magnetosheath. If these magnetic field fluctuations are a possible source for the wavy velocity variations, there can be some relationship between these magnetic field fluctuations and wavy velocity variations at the inner edge of LLBL. After the interval during which the wavy variations were observed, the wavy velocity variations in the magnetosphere were absent, and no simultaneous fluctuations of the magnetic field were observed in the magnetosheath. From these observations, we can easily predict that some relationship between the magnetosheath magnetic field fluctuations and wavy velocity variations is expected.

[25] We, then, examined the relationship between the wavy plasma velocity and simultaneous dynamic, magnetic, and plasma pressures as proxies of energy with the magnetic field and plasma during the interval of 6 min between 0435 and 0441 UT, shown in Figure 7. From top to bottom, the V_x and V_y components observed by THEMIS C, D and E in the magnetosphere, the plasma density (N_p), the temperature (T), the dynamic (Pd), the magnetic (Pb) and plasma (Pg) pressures obtained by THEMIS B in the magnetosheath are presented. The dynamic ($\frac{1}{2}mN_pV_t^2$), magnetic ($\frac{1}{2}\mu_0B_t^2$) and plasma ($N_p kT$) pressures are computed using the magnetic field and plasma parameters from THEMIS B. The plasma density, the temperature and the plasma pressures enhanced when simultaneous plasma velocities increased as shown with black vertical lines. The values of the dynamic pressure were much smaller than those of both the magnetic and plasma pressures.

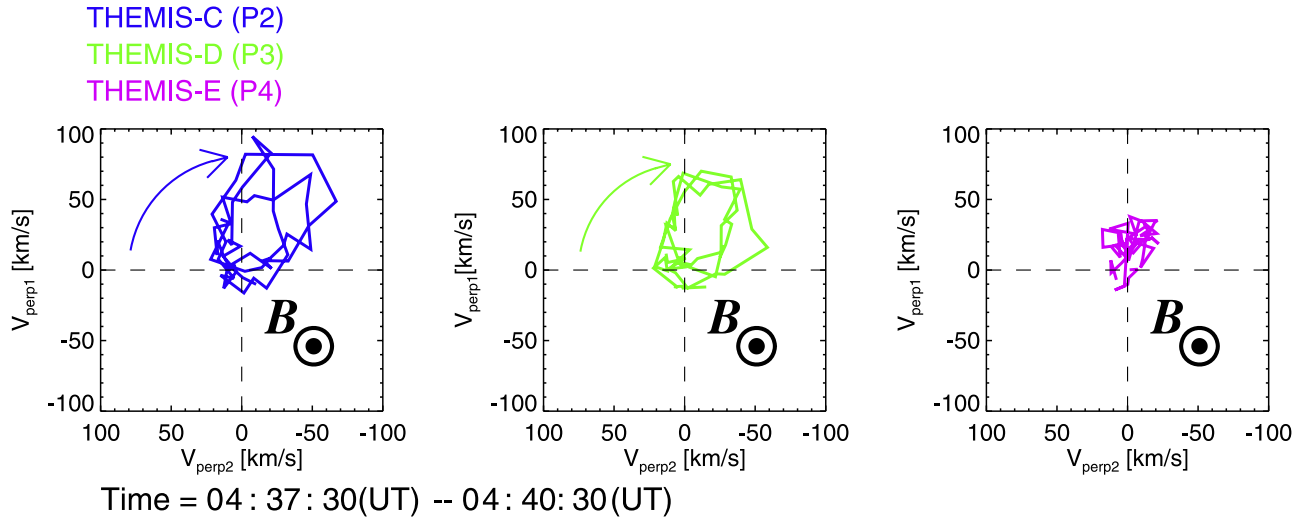


Figure 6. The velocity hodograms during the interval of 2.5 min between 0437:30 and 0440:30 UT are drawn on the plane of the velocities perpendicular to the local magnetic field line ($V_{\text{perp1}}-V_{\text{perp2}}$ plane). During this interval, the clearest wavy variations have been observed in the plasma velocity. (left to right) The velocity hodograms obtained by THEMIS C, D, and E are presented. The magnetic field direction is from the paper to the reader, and the direction of the hodogram's polarization is shown with bent arrows.

Furthermore, the magnetosheath dynamic pressure varied with the in-phase to the plasma density, temperature and the plasma pressure until about 0439 UT, but it became closer to 0.0 nPa after 0439 UT when the plasma velocity variations appeared very clearly. This very small variation of the magnetosheath dynamic pressure was consistent with the stable solar wind dynamic pressure during which THEMIS B observed the mirror mode waves in the magnetosheath. Therefore, these results suggest that neither the magnetosheath nor the solar wind dynamic pressures contribute to an excitation of these wavy plasma velocity variations observed at the inner edge of LLBL. The magnetic pressure decreases at this time. However, the periodicities of the variations of all parameters were between 0.5 minute and 1 minute. The similarity of the period at all four THEMIS probes suggests that the magnetic field fluctuations observed in the magnetosheath are a possible source for the wavy velocity variations at the inner edge of LLBL.

[26] The periodicity of the wavy velocity was clearly consistent with that of the magnetic/plasma pressure variations. The correlations between these also show the in phase or out of phase. However, in general, the fluctuations in the magnetosheath cannot directly propagate or be transmitted into the magnetosphere because only fast-mode and Alfvén mode waves are able to propagate or transmit into the magnetosphere. In this case, at the inner edge of LLBL, complicated mixed mode waves, having dominant Alfvénic structure were observed.

[27] Therefore, the wavy plasma velocity variations were response of the plasma in the magnetospheric side to the magnetic field fluctuations in the magnetosheath. This magnetic field fluctuations observed in the magnetosheath must drive the magnetopause surface waves, which in turn launch fast or Alfvén mode waves in the magnetosphere. However, we cannot obtain the clear evidence that these launched fast or Alfvén mode waves were propagating

through the magnetosphere and THEMIS C and D directly observed these waves.

7.2. A Possible Cause for the Magnetosheath Magnetic Field Fluctuations

[28] Next, we consider a possible cause for these magnetic field periodic fluctuations observed by THEMIS B. As possible mechanisms to cause these fluctuations, we can consider the mirror mode waves in the magnetosheath close to the magnetopause. The energy with the mirror mode waves occurring in the magnetosheath close to the magnetopause can contribute to the power of the other mode waves [Song *et al.*, 1992a, 1992b]. In this case, the possible mirror mode waves induce the magnetopause surface waves to launch the fast and Alfvén mode waves into the magnetosphere.

[29] In order to identify whether these fluctuations are mirror mode waves or not, we applied the criterion proposed by Hasegawa [1969] to this case. This criterion is given by

$$1 + \beta_{\perp} \left(1 - \frac{T_{\perp}}{T_{\parallel}} \right) < 0. \quad (1)$$

[30] Figure 8 shows a plot of the values of the ion anisotropy, together with the magnetic, plasma and total pressures obtained from THEMIS B. From top to bottom, the magnetic, plasma and total pressures, β value perpendicular to the magnetic field line ($\beta_{\perp} = \frac{N_p k T_{\perp}}{\frac{1}{2} \mu_0 B_{\perp}^2}$), the values for the condition of an excitation of the mirror mode waves (MMW condition) which are obtained with the equation (1), and the ion anisotropy values during the 42 min between 0429 and 0511 UT are presented. The durations during which THEMIS B observed and did not observe the magnetosheath mirror modes were between 0430:00 and

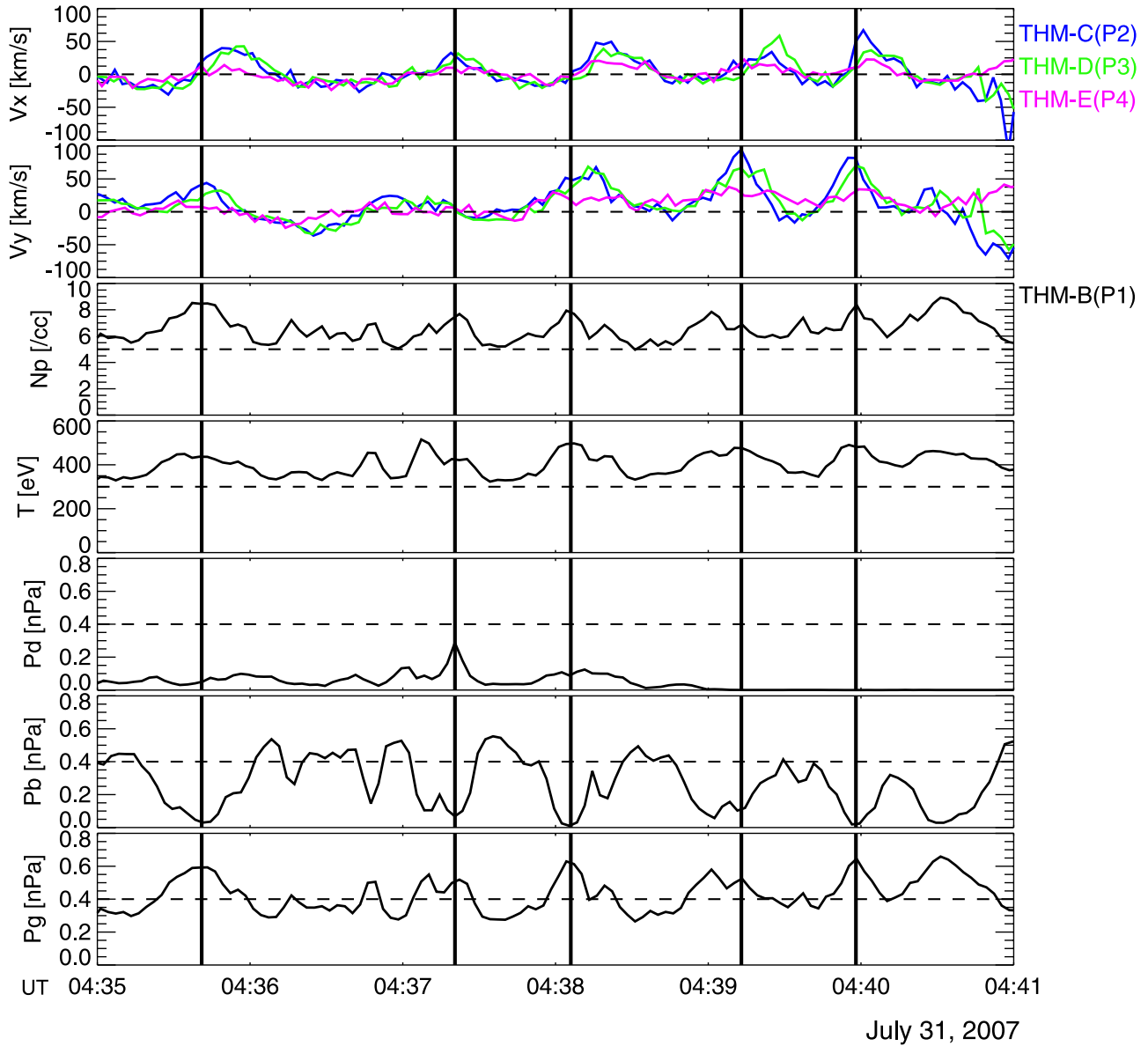


Figure 7. Plots of the V_x and V_y components observed by THEMIS C, D, and E and the plasma density; the temperature; and the dynamic, magnetic, and plasma pressures obtained from THEMIS B are presented. The dynamic ($\frac{1}{2}mN_pV_i^2$), magnetic ($\frac{1}{2}\mu_0B_i^2$), and plasma ($N_p kT$) pressures are computed using the magnetic field and plasma parameters from THEMIS B. The interval of this plot is 6 min between 0435 and 0441 UT. Black vertical lines show the in-phase or out-of-phase relations among the plasma velocity; the plasma density; the temperature; and the dynamic, magnetic, and plasma pressures.

0443:14 UT, and between 0449:10 and 0510:10 UT, bracketed by two black and two gray vertical dotted lines, respectively. We were not able to plot the values of β_{\perp} , MMW condition and ion anisotropy after 0501 UT because of a lack of T_{\parallel} and T_{\perp} data. During the interval of the mirror mode wave, the magnetic and plasma pressures were in antiphase. Associated total pressure also varied periodically, but its background value was nearly constant (about 0.75 nPa). The value for β perpendicular to the magnetic field line ranged from 0.2 to 2.0 in the low-energy plasma (low plasma pressure) regions to values above 5.0 and sometimes ranged above 20.0 in the high plasma pressure regions. The corresponding values of MMW condition in both the low-energy plasma and low β_{\perp} regions were

almost between 0.0 and 0.5, and sometimes those were negative (~ -0.1). From this result only, an excitation of mirror mode waves seems to be hard in both low-energy plasma and low β_{\perp} regions because the criteria are not fully satisfied. The values for MMW condition were negative in both the high plasma pressure and β_{\perp} regions, and resultant mirror mode waves are likely to be excited. The value of the ion anisotropy ($\frac{T_{\perp}}{T_{\parallel}} - 1.0$) fluctuated considerably, but the background value was about 0.8, indicating that T_{\perp} was about twice as large as T_{\parallel} in the magnetosheath. Large amplitude perturbations were present during an interval when the background plasma in the low plasma pressure region was stable. This fact suggests that the waves were generated elsewhere and connected to the point of

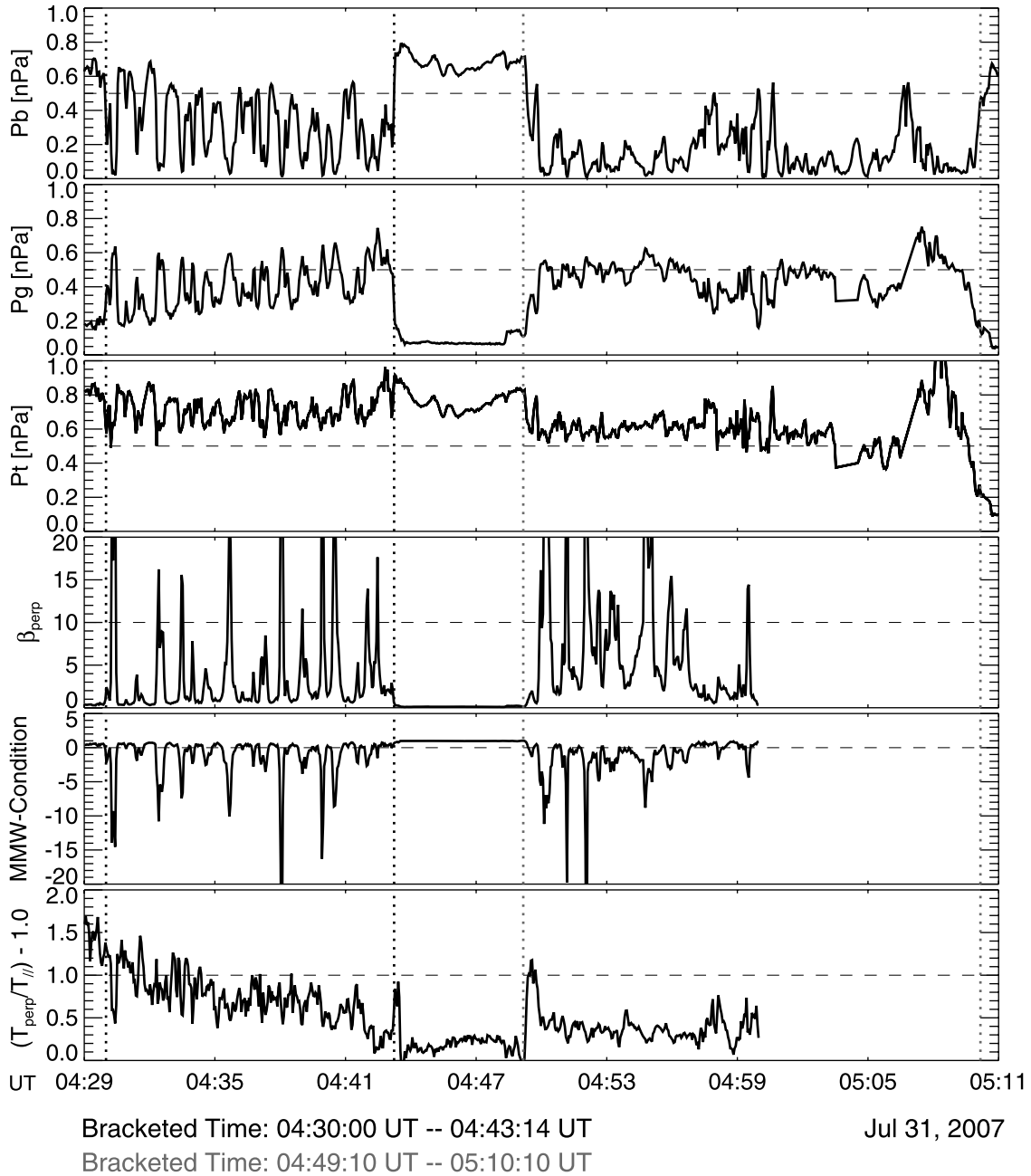


Figure 8. Result of the criteria to identify the mirror mode waves, proposed by *Hasegawa* [1969], is presented. The criteria to identify the mirror mode waves are plotted together with the magnetic, plasma, and total pressures obtained from THEMIS B. From top to bottom, the magnetic, plasma, and total pressures; β value perpendicular to the magnetic field line calculated with the equation of $(\frac{N_p k T_{\perp}}{2 \mu_0 B^2})$; the values for the condition of an excitation of the mirror mode waves (MMW condition) which are obtained with the equation (1); and the values of the ion anisotropy during 42 min between 0429 and 0511 UT are presented. After 0501 UT, the values of β_{\perp} , MMW condition, and ion anisotropy were not plotted because of a lack of T_{\parallel} and T_{\perp} data. The magnetosheath intervals with and without the mirror mode waves are bracketed with two black and two gray vertical dotted lines drawn between 0430:00 and 0434:14 UT and between 0449:10 and 0510:10 UT, respectively.

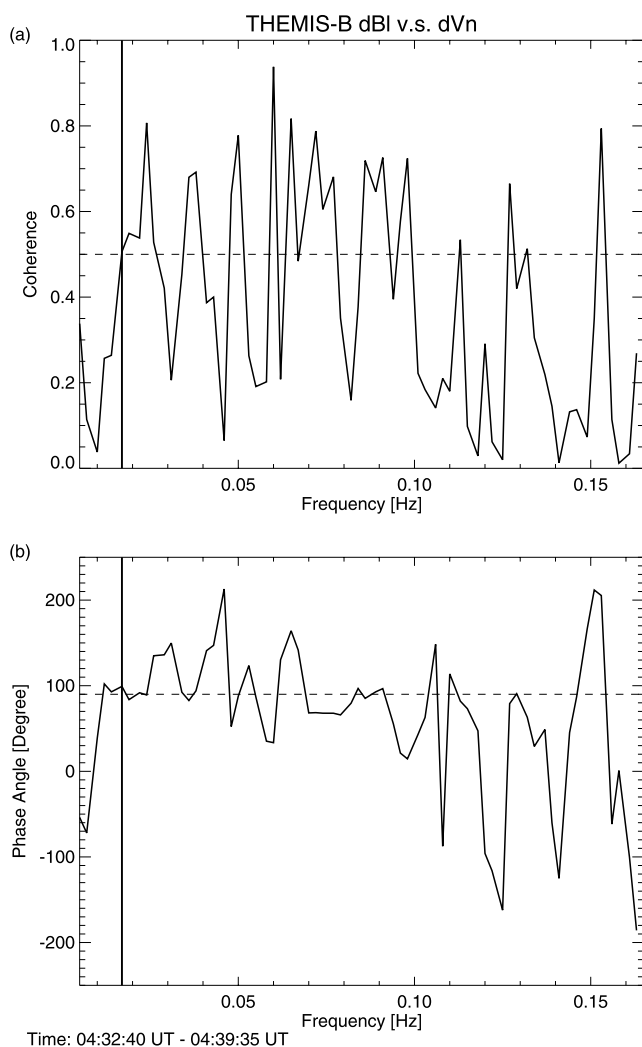


Figure 9. (a) The coherence and (b) the phase angle of the variations between the approximate north–south magnetic field component (B_1) and the plasma velocity component normal to the magnetopause surface (V_n) in the magnetosheath during about 7 min between 0432:40 and 0439:35 UT were plotted against the wave frequency. The coordinate system in the magnetic field and plasma velocity was transferred from GSM to LMN using minimum variance analysis. The value of 0.5 in the coherence and 90° phase angle for thresholds of good correlation between the magnetic field and plasma velocity are shown with horizontal dashed lines in both Figures 9a and 9b.

observations. Their amplitudes presumably grew during the convection because criteria for the mirror mode waves were satisfied even in the high plasma pressure regions.

[31] During the next magnetosheath interval between 0449:10 and 0510:10 UT, the wavy variations were not observed in both the magnetic and plasma pressures, although the clear anticorrelation between them was found. The variations of β_\perp and MMW condition values were almost the same as those in the previous magnetosheath interval. However, the total pressure variations were much smaller, and the average ion anisotropy value was about 0.3,

which was also smaller than that in the previous magnetosheath interval. From these results, it can be harder to consider that the mirror mode waves occurred during this magnetosheath interval.

[32] These large differences of the total pressure variation and the average ion anisotropy value, which becomes one of the conditions for an excitation of the mirror mode waves, between in the magnetosheath with and without the mirror mode waves might come from the difference of the IMF B_z polarity. In the magnetosheath with the mirror mode waves, the IMF B_z was positive, but was almost negative in the magnetosheath without the mirror mode waves. Under the positive and negative IMF B_z , the magnetosheath conditions, that is, the configurations of the magnetic field lines in the magnetosheath adjacent to the magnetopause, and the magnetopause behavior would change drastically. Therefore, the difference of the magnetosheath conditions controls an existence/an absence of the mirror mode waves in the magnetosheath. Furthermore, the obtained evidence for an existence of the mirror mode waves simultaneously supports that the Alfvénic variations observed in the LLBL are strongly related to the magnetosheath mirror mode waves, because no Alfvénic responses were found in both the magnetic field and plasma again without the mirror mode waves during another magnetosheath interval.

[33] As a double check for whether mirror mode waves can be developed well, we examined the phase difference between the magnetic field and plasma velocity perturbations using the techniques proposed by *Lin et al.* [1998]. The unique character for mirror mode waves is that a 90° phase difference between the magnetic field and the plasma velocity variations exists together with a 180° phase difference between the magnetic field strength and the plasma density. In this magnetosheath, a clear anticorrelation between the magnetic field strength and the plasma number density was seen, and simultaneous magnetic field and plasma pressure also show the anticorrelated variations each other. Therefore, a 180° phase difference exists between the magnetic field strength and the plasma number density. Next, the correlation between the perturbations of the magnetic field and plasma velocity was examined. Figure 9 shows the coherence (Figure 9a) and the phase angle (Figure 9b) of the variations between approximate north–south component (B_1) and plasma velocity normal to the magnetopause surface (V_n), when THEMIS B observed the magnetosheath during about 7 min between 0432:40 and 0439:35 UT. The coordinated system of the magnetic field and plasma velocity are transferred from GSM to LMN using minimum variance analysis [Sonnerup and Cahill, 1967]. During the interval, the coefficient of coherence between dB_1 and dV_n is almost above 0.5 shown with the horizontal dashed line in Figure 9a. The phase angle was found to fluctuate as presented in Figure 9b, but its average value for frequency range less than 0.1 Hz was almost 90° as shown with horizontal dashed line. Furthermore, at the common dominant frequency (about 17.0 mHz) as shown with vertical solid lines, the coherence and corresponding phase angle between the magnetic field and plasma velocity variations were 0.51 and 98° , respectively. Therefore, these conditions of the perturbations of the magnetic field and plasma velocity, observed in the magnetosheath are consis-

tent with the expectations for an excitation of mirror mode wave.

[34] The IMF wavy structures, which can be an origin of the magnetosheath mirror mode waves were not detected by ACE, located on the Sun-Earth line. The simultaneous WIND spacecraft was located in the dawnside far off from the Sun-Earth line. We found the weak peaks in the IMF intensity, the number density and the dynamic pressure spectra, which were calculated using the magnetic field and plasma data from WIND. Furthermore, these peaks had the same periodicity range (0.5 minute \sim 1 minute) as those of the magnetosheath mirror mode waves. However, it is difficult to elucidate whether these weak compressional/slow mode structures in the solar wind directly initiate the magnetosheath mirror mode waves. Because these structures were observed by a single spacecraft, the wave number vector that shows which direction the wave structures are traveling cannot be obtained.

8. Conclusions

[35] With the unique simultaneous observations by a string-of-pearls configuration of the THEMIS spacecraft, Alfvénic variations in the plasma velocity are observed at the inner edge of LLBL, and are induced by the mirror mode waves in the magnetosheath. THEMIS C, D and E observed the clear wavy variations in both the V_x and V_y components, and the magnetic field also varied with the same dominant frequency and ellipticity at the inner edge of LLBL. Furthermore, a correlation between the magnetic field and wavy velocity variations was in phase. However, there were no particular periodic variations in both the plasma density and the temperature. The magnetic field variations were independent on the variations of the plasma number density. In THEMIS C and D observations, the vortex-like structures in the plasma velocity hodograms are clearly found on the plane of the velocities perpendicular to the magnetic field line. From these results, the wavy variations observed by THEMIS C and D have complicated mixed mode structure, but their dominant wave characteristics are Alfvénic. On the other hand, the velocity hodogram obtained from THEMIS E did not present the clear vortex-like structures even though THEMIS E also observed the wavy velocity variations at the inner edge of LLBL as well as THEMIS C and D. Therefore, these Alfvénic responses were observed by THEMIS C and D in the narrow region, and another waves without dominant Alfvénic characteristics can be detected by THEMIS E.

[36] THEMIS B simultaneously observed the mirror mode waves in the magnetosheath. The magnetopause surface waves can be induced by this mirror mode waves because a periodicity of the antiphase relation between the magnetic and plasma pressures observed in the magnetosheath was consistent with that of the wavy velocity variations at the inner edge of LLBL. Namely, the anticorrelation between the magnetic and plasma pressures is produced by an excitation of the mirror mode waves, and resultant magnetopause undulations are induced. The perturbations in the magnetosheath cannot directly propagate/transmit into the magnetosphere because only fast and Alfvén mode waves theoretically are allowed to travel into the magnetosphere. Therefore, the surface waves were

induced by the magnetopause undulations, and resultant magnetic field and plasma responses in the magnetospheric side are observed by the THEMIS satellite.

[37] On the basis of our results, we can provide a global picture of responses for the magnetic field and plasma from the magnetosheath to the magnetosphere by unique simultaneous observations made by THEMIS. These observations reveal that waves are induced by the undulations of the dayside magnetopause near the subsolar region under the IMF direction is northward, and resultant magnetic field and plasma Alfvénic responses are observed at the inner edge of LLBL. These results are direct evidence that the energy originated from the magnetosheath is certainly transmitted and transported into the magnetosphere via magnetopause surface waves.

[38] **Acknowledgments.** This work was supported in part by National Science Council grant NSC-96-2811-M-008-002 and National Space Organization grant 97-NSPO(B)-SP-FA07-01 to National Central University and in part by Ministry of Education under the Aim for Top University program at National Central University. M.N. thanks J. P. McFadden for helpful comments and suggestions on this manuscript and L.-S. Lyu for fruitful discussions and comments on the initial stage of this study. THEMIS was supported under NASA NASS-02099. We also thank N. F. Ness and D. J. McComas for the use of ACE magnetic field and plasma data and R. P. Lepping and K. W. Ogilvie for the use of WIND magnetic field and plasma data via Coordinated Data Analysis Web site provided by NASA/GSFC.

[39] Zuyin Pu thanks R. L. Kessel for her assistance in evaluating this paper.

References

- Angelopoulos, V. (2008), The THEMIS mission, *Space Sci. Rev.*, *141*, 5–34, doi:10.1007/s11214-008-9336-1.
- Auster, H. U., et al. (2008), The THEMIS fluxgate magnetometer, *Space Sci. Rev.*, *141*, 235–264, doi:10.1007/s11214-008-9365-9.
- Cattaneo, M. B. B., C. Basile, G. Moreno, and J. D. Richardson (1998), Evolution of mirror structures in the magnetosheath of Saturn from the bow shock to the magnetopause, *J. Geophys. Res.*, *103*(A6), 11,961–11,972.
- Glassmeier, K.-H., et al. (2008), Magnetospheric quasi-static response to the dynamic magnetosheath: A THEMIS case study, *Geophys. Res. Lett.*, *35*, L17S01, doi:10.1029/2008GL033469.
- Hasegawa, A. (1969), Drift mirror instability in the magnetosphere, *Phys. Fluids*, *12*(12), 2642–2650.
- Hsu, T.-S., and R. L. McPherron (2003), Occurrence frequencies of IMF triggered and nontriggered substorms, *J. Geophys. Res.*, *108*(A7), 1307, doi:10.1029/2002JA009442.
- Joy, S. P., M. G. Kivelson, R. J. Walker, K. K. Khurana, C. T. Russell, and W. R. Paterson (2006), Mirror mode structures in the Jovian magnetosheath, *J. Geophys. Res.*, *111*, A12212, doi:10.1029/2006JA011985.
- Kessel, R. L. (2008), Solar wind excitation of Pc5 fluctuations in the magnetosphere and on the ground, *J. Geophys. Res.*, *113*, A04202, doi:10.1029/2007JA012255.
- Kim, K.-H., C. A. Cattell, D.-H. Lee, K. Takahashi, K. Yumoto, K. Shiokawa, F. S. Mozer, and M. Andre (2002), Magnetospheric responses to sudden and quasiperiodic solar wind variations, *J. Geophys. Res.*, *107*(A11), 1406, doi:10.1029/2002JA009342.
- Kivelson, M. G., and C. T. Russell (1995), *Introduction to Space Physics*, Cambridge Univ. Press, New York.
- Kivelson, M. G., and D. J. Southwood (1991), Ionospheric traveling vortex generation by solar wind buffeting of the magnetosphere, *J. Geophys. Res.*, *96*(A2), 1661–1667.
- Lin, C.-H., J.-K. Chao, L.-C. Lee, D.-J. Wu, Y. Li, B.-H. Wu, and P. Song (1998), Identification of mirror waves by the phase difference between perturbed magnetic field and plasmas, *J. Geophys. Res.*, *103*(A4), 6621–6631.
- Lucek, E. A., M. W. Dunlop, A. Balogh, P. Cargill, W. Baumjohann, E. Georgescu, G. Haerendel, and K.-H. Fornacon (1999a), Mirror mode structures observed in the dawn-side magnetosheath by Equator-S, *Geophys. Res. Lett.*, *26*(14), 2159–2162.
- Lucek, E. A., M. W. Dunlop, A. Balogh, P. Cargill, W. Baumjohann, E. Georgescu, G. Haerendel, and K.-H. Fornacon (1999b), Identification of magnetosheath mirror modes in Equator-S magnetic field data, *Ann. Geophys.*, *17*, 1560–1573.

- Lucek, E. A., M. W. Dunlop, T. S. Horbury, A. Balogh, P. Brown, P. Cargill, C. Carr, K.-H. Fornacon, E. Georgescu, and T. Oddy (2001), Cluster magnetic field observations in the magnetosheath: Four-point measurements of mirror structures, *Ann. Geophys.*, *19*, 1421–1428.
- Matsuoka, H., K. Takahashi, K. Yumoto, B. J. Anderson, and D. G. Sibeck (1995), Observation and modeling of compressional Pi 3 magnetic pulsations, *J. Geophys. Res.*, *100*(A7), 12,103–12,115.
- McFadden, J. P., C. W. Carlson, D. Larson, M. Ludlam, R. Abiad, B. Elliott, P. Turin, M. Marckwordt, and V. Angelopoulos (2008), The THEMIS ESA plasma instrument and in-flight calibration, *Space Sci. Rev.*, *141*, 277–302.
- Sakurai, T., Y. Tonegawa, T. Kitagawa, K. Yumoto, T. Yamamoto, S. Kokubun, T. Mukai, and K. Tsuruda (1999), Dayside magnetopause Pc 3 and Pc 5 ULF waves observed by the GEOTAIL satellite, *Earth Planets Space*, *51*(9), 965–978.
- Sibeck, D. G., W. Baumjohann, and R. E. Lopez (1989a), Solar wind dynamic pressure variations and transient magnetospheric signatures, *Geophys. Res. Lett.*, *16*(1), 13–16.
- Sibeck, D. G., et al. (1989b), The magnetospheric response to 8-minute period strong-amplitude upstream pressure variations, *J. Geophys. Res.*, *94*(A3), 2505–2519.
- Song, P., C. T. Russell, and M. F. Thomsen (1992a), Slow mode transition in the frontside magnetosheath, *J. Geophys. Res.*, *97*(A6), 8295–8305.
- Song, P., C. T. Russell, and M. F. Thomsen (1992b), Waves in the inner magnetosheath: A case study, *Geophys. Res. Lett.*, *19*(22), 2191–2194.
- Sonnerup, B. U. Ö., and L. J. Cahill Jr. (1967), Magnetopause structure and attitude from Explorer 12 observations, *J. Geophys. Res.*, *72*(1), 171–183.
- Tsurutani, B. T., E. J. Smith, R. R. Anderson, K. W. Ogilvie, J. D. Scudder, D. N. Baker, and S. J. Bame (1982), Lion roars and nonoscillatory drift mirror waves in the magnetosheath, *J. Geophys. Res.*, *87*(A8), 6060–6072.
- Violante, L., B. M. B. Cattaneo, G. Moreno, and J. D. Richardson (1995), Observations of mirror waves and plasma depletion layer upstream of Saturn's magnetopause, *J. Geophys. Res.*, *100*(A7), 12,047–12,055.
-
- V. Angelopoulos, Institute of Geophysics and Planetary Physics, University of California, Los Angeles, CA 90095, USA. (vassilis@igpp.ucla.edu)
- H.-U. Auster, Institut für Geophysik und Extraterrestrische Physik, Technische Universität, Mendelssohnstraße 3, D-38106 Braunschweig, Germany. (uli.auster@tu-bs.de)
- C. W. Carlson, Space Sciences Laboratory, University of California, 7 Gauss Way, Berkeley, CA 94720-7450, USA. (cwc@ssl.berkeley.edu)
- C.-H. Lin, Department of Electrical Engineering, Ching Yun University, Jhongli, Taoyuan 32097, Taiwan. (chlin@cyu.edu.tw)
- M. Nowada and J.-H. Shue, Institute of Space Science, National Central University, Jhongli, Taoyuan 32001, Taiwan. (nowada@jupiter.ss.ncu.edu.tw; jhshue@jupiter.ss.ncu.edu.tw)
- T. Sakurai, Department of Aeronautics and Astronautics, Tokai University, 1117 Kitakaname, Hiratsuka, Kanagawa, 259-1292, Japan. (tohrusakurai@gmail.com)
- D. G. Sibeck, NASA Goddard Space Flight Center, Code 674, Greenbelt, MD 20771, USA. (david.g.sibeck@nasa.gov)